Received: 27 November 2020 | Revised: 16 March 2021

DOI: 10.1111/liv.14888

ORIGINAL ARTICLE

Liver INTERNATIONAL WILEY

Elafibranor and liraglutide improve differentially liver health and metabolism in a mouse model of non-alcoholic steatohepatitis

Nikolaos Perakakis[1] | Konstantinos Stefanakis[1] | Michael Feigh[2] | Sanne S. Veidal[2] | Christos S. Mantzoros[1]

[1]Department of Medicine, Boston VA Healthcare System and Beth Israel Deaconess Medical Center, Harvard Medical School, Boston, MA, USA

[2]Gubra, Hørsholm, Denmark

Correspondence
Christos S. Mantzoros, Department of Medicine, Boston VA Healthcare System and Beth Israel Deaconess Medical Center, Harvard Medical School, 330 Brookline Avenue, East Campus, Beth Israel Deaconess Medical Center, ASN-249, Boston, MA 02215, USA.
Email: cmantzor@bidmc.harvard.edu

Funding information
The current work was an investigator-initiated study funded by Coherus Biosciences through a grant provided to CSM through BIDMC. CSM was also funded by NIH K24DK081913. NiP was funded by the Deutsche Forschungsgemeinschaft (DFG, German Research Foundation)—PE2431/3-1:1.

Handling Editor: Michelle Long

Abstract

Background & Aims: This study aimed to assess and compare the effects of the GLP-1 analog liraglutide and the PPARα/δ agonist elafibranor on liver histology and their impact on hepatic lipidome, metabolome, Kupffer and hepatic stellate cell activation in a model of advanced non-alcoholic fatty liver disease (NAFLD).

Methods: Male C57BL/6JRj mice with biopsy-confirmed hepatosteatosis and fibrosis induced by 36-week Amylin liver NASH (AMLN) diet (high-fat, fructose and cholesterol) were randomized to receive for 12 weeks: (a) liraglutide (0.4 mg/kg/day s.c.), (b) elafibranor (30 mg/kg/day p.o.) and (c) vehicle. Metabolic status, liver pathology, markers of inflammation, Kupffer and stellate cell activation, and metabolomics/lipidomics were assessed at study completion.

Results: Elafibranor and liraglutide improved weight, insulin sensitivity, glucose homeostasis and NAFLD activity score (pre-to-post biopsy). Elafibranor had a profound effect on hepatic lipidome, demonstrated by reductions in glycerides, increases in phospholipids, and by beneficial regulation of mediators of fatty acid oxidation, inflammation and oxidative stress. Liraglutide had a major impact on inflammatory and fibrogenic markers of Kupffer and hepatic stellate cell activation (Galectin-3, Collagen type I alpha 1, alpha-smooth muscle actin). Liraglutide exerted beneficial effects on bile acid and carbohydrate metabolism, demonstrated by restorations of the concentrations of bile acids, glycogen metabolism by-products and pentoses, thus facilitating glycogen utilization turnover and nucleic acid formation.

Conclusions: Liraglutide and elafibranor robustly but through different pathways improve overall metabolic health and liver status in NAFLD. These data indicate important differences in the respective mechanisms of action and support the notion for their evaluation as combination therapies in the future.

Abbreviations: 5-MeTHF, 5-methyltetrahydrofolate; ALT, alanine aminotransferase; AST, aspartate aminotransferase; CE, cholesterol ester; Col1a1, collagen 1a1; DAG, diacylglycerol; DiHOME, dihydroxyoctadecenoic acid; DIO, diet-induced-obese; EPA, eicosapentaenoic acid; FA, fatty acids; FXR, farnesoid X receptor; Gal-3, galectin-3; GLP-1, glucagon-like peptide 1; GLP-1, glucagon-like peptide 1; GLP-1RA, glucagon-like peptide 1 receptor agonists; GSH, glutathione; GSHNE, glutathione-4-hydroxynonenal; HODE, hydroxyoctadecadienoic acid; HP, hydroxyproline; IHC, immunohistochemistry; ipITT, intraperitoneal insulin tolerance test; MAG, monoacylglycerol; NAFL, non-alcoholic fatty liver; NAFLD, non-alcoholic fatty liver disease; NASH, non-alcoholic steatohepatitis; OGTT, oral glucose tolerance test; PC, phosphatidylcholine; PE, phosphatidylethanolamines; PG, prostaglandin; PPARα, peroxisome proliferator-activated receptor alpha; PPARα/δ, peroxisome proliferator-activated receptor alpha/delta; RCT, randomized clinical trial; SAH, S-adenosylhomocysteine; SAM, S-adenosylmethionine; SAMa, significance analysis of microarrays; s-PLS-DA, sparse partial least squares-discriminant analysis; SPM, specialized pro-resolving mediator; TAG, triacylglycerol; TC, total cholesterol; TCA, tricarboxylic acid; TG, triglycerides; UDP, uridine diphosphate; VLDL, very low- density lipoprotein; α-SMA, alpha-smooth muscle actin.

KEYWORDS
GLP-1, lipidomics, metabolomics, NAFLD, PPARa/d, PPARγ, steatosis

Key points

- In a diet-induced-obese mouse model of advanced non-alcoholic fatty liver disease (NAFLD), we investigated the metabolic, histological, metabolomic and lipidomic effects of liraglutide, a glucagon-like peptide-1 receptor agonist and elafibranor, a dual peroxisome proliferator-activated receptor alpha-delta agonist.
- While both regimens improved liver histology, glucose regulation and metabolic indices, elafibranor robustly affected lipid and antioxidant metabolism, while liraglutide chiefly improved carbohydrate and bile acid utilization and reduced immunohistochemical markers of hepatic damage.
- Thus, the two agents diverge in their mechanistic treatment of advanced NAFLD pathology, supporting their combinatory evaluation.

1 | INTRODUCTION

Non-alcoholic fatty liver (NAFL) disease (NAFLD) is a metabolic disease characterized by increasing prevalence, currently affecting 20%-30% of the general population.[1] NAFLD remains an unmet clinical need, and thus, numerous studies are currently underway to evaluate the efficacy and safety of several different drug candidates.[2,3] NAFLD is characterized initially by increased lipid accumulation in the liver (NAFL) that can progress to non-alcoholic steatohepatitis (NASH) and later to liver fibrosis and cirrhosis. Most studies specifically focus on NASH with liver fibrosis because this stage of the disease is strongly related to increased hepatic- and cardiovascular-related mortality.

Current therapeutic approaches involve both the investigation of already licensed medications for the treatment of metabolic diseases, especially type 2 diabetes mellitus or obesity,[2,4,5] and the evaluation of novel medications with liver-specific effects.[2,6] These efforts are supported by extensive data from pathophysiological studies showing a causal relationship between insulin resistance, hyperglycaemia, obesity and the development of NASH.[1,7] Glucagon-like peptide 1 (GLP-1) receptor analogs, such as liraglutide and semaglutide are widely used for the treatment of type 2 diabetes and obesity and the latter recently received break through designation from the Food and Drug Administration (FDA) for the treatment of NASH.[4,5] Similarly, elafibranor, a dual peroxisome proliferator-activated receptor α (PPARα) and PPARδ agonist, is currently being evaluated in clinical trials in humans. Both liraglutide and elafibranor have shown beneficial effects in the treatment of NASH in animal models,[8-13] and it is thus anticipated that some of these effects would be also observed in humans.[14-21] Additionally, it is becoming increasingly evident that due to the involvement of multiple metabolic and hepatic factors in NASH pathogenesis and progression, different medications may be affecting different metabolic or molecular pathways. Thus, because one medication may not be able to reverse the course of the disease, and a combination of treatments may eventually be needed,[22] the specific molecular, metabolic and metabolomic pathways affected by each medication need to be studied in head-to-head studies. This will enable to identify, directly compare and contrast the mechanisms of action of important drug candidates for NASH. Consequently, it will not only allow us to assess which patients are most likely to profit from each medication but also to predict which combinations of treatments may be particularly beneficial for a patient through the restoration of multiple mechanistic pathways.

Previous studies have shown that profound perturbations in hepatic metabolome and lipidome are observed in NASH and are causally related to disease pathogenesis and progression.[23-25] These perturbations may elucidate the development of non-invasive tests for the diagnosis and staging of NASH or pinpoint targets for the development of effective treatments.[23,24,26,27] Additionally, it is known that the activation of Kupffer cells and subsequently of hepatic stellate cells are key components of the transition from hepatic steatosis to steatohepatitis and liver fibrosis.[28,29] We hypothesized that liraglutide, which is a medication that acts both in the brain and in the periphery to improve glucose homeostasis and energy intake, will affect hepatic function through distinct mechanisms compared with elafibranor, which is a medication that acts directly on the liver. In this context, our study aimed to investigate and compare for the first time in parallel how liraglutide and elafibranor affect liver histology and which is their impact on hepatic metabolome and lipidome as well as on markers of hepatic Kupffer and stellate cell activation in a biopsy-proven mouse model of advanced NAFLD with hepatic inflammation and fibrosis.

2 | METHODS

2.1 | Ethics

All animal experiments were conducted in accordance with Gubra bioethical guidelines, which are fully compliant with internationally accepted principles for the care and use of laboratory animals.

2.2 | Study design

The study design and methodology have been previously described[6] (Figure 1). Briefly, male C57BL/6JRj mice were fed AMLN diet (40% fat with 20% trans-fat, 2% cholesterol and 22% fructose, D09100301, Research Diets Inc, Table S1) for 36 weeks prior to study start, and with liver pre-biopsy collected at −3 weeks for study inclusion based on steatosis score ≥2 and fibrosis score ≥1 according to criteria by Kleiner et al,[30] were randomized to receive for 12 weeks: (a) vehicle (n = 13, diet-induced-obese [DIO]-NASH), (b) liraglutide 0.4 mg/kg/day s.c. (n = 14, DIO-NASH + liraglutide), (c) elafibranor 30 mg/kg/day p.o. (n = 13, DIO-NASH + elafibranor) (see Supporting Information for justification of dose and duration of treatment). A fourth group was included in the study that consisted of control mice of similar age that were fed normal chow and did not develop NASH (n = 12, chow + vehicle).

2.3 | Tolerance tests and biochemical measurements

In the seventh week of treatment, an oral glucose tolerance test (OGTT, with 2 g/kg glucose per os) and, in the 10th week of treatment, an intraperitoneal insulin tolerance test (ipITT, with 0.5 U/kg Novorapid) were performed after a 6-hour fast. Glucose was assessed at 0, 15, 30, 60 and 120 minutes of the OGTT and ipITT. Details on the tests have been previously described.[6] Plasma alanine aminotransferase (ALT), aspartate aminotransferase (AST), total cholesterol (TC), triglycerides (TGs) and urea as well as hepatic TC and TG (after sample homogenization, extraction with NP-40 by heating to 90°C and centrifugation) were measured with an automated analyser (Cobas c501, Roche Diagnostics). Mouse insulin was measured with the MSD Platform (Meso Scale Diagnostics). Hepatic hydroxyproline (HP) was assessed with a colorimetric assay (QuickZyme Biosciences) in the supernatant of previously homogenized, hydrolysed and centrifuged liver samples.

2.4 | Liver pathology and immunohistochemistry staining

Details about both procedures have been previously described and are also largely included in Supplemental Material.[6] Both liver biopsies (at baseline and treatment completion) were stained with haematoxylin–eosin and Picrosirius red, and scored according to Kleiner et al[30] by a histopathology specialist who was blinded for the study groups. Quantitative assessment of steatosis in haematoxylin–eosin stained slides, of Galectin-3 (Gal-3; Ab from Biolegend, Cat. #125402), alpha-smooth muscle actin (α-SMA; Ab from Abcam, Cat. #Ab124964) and collagen 1a1 (Col1a1; Ab from Southern Biotech, Cat. #1310-01) in immunohistochemistry (IHC)-stained slides was performed with image analysis by the Visiomorph software (previously published information in supplementary appendix of Perakakis et al[6]).

2.5 | EchoMRI body composition

Murine body composition was assessed by an EchoMRI 3-1 Body composition analyser (EchoMRI, USA) in non-anaesthetized mice and is presented as water, fat and fat-free mass.

2.6 | Metabolomics–lipidomics

Metabolomics and lipidomics mass-spectrometric analysis and data curation was performed by Metabolon Inc, and the methodology

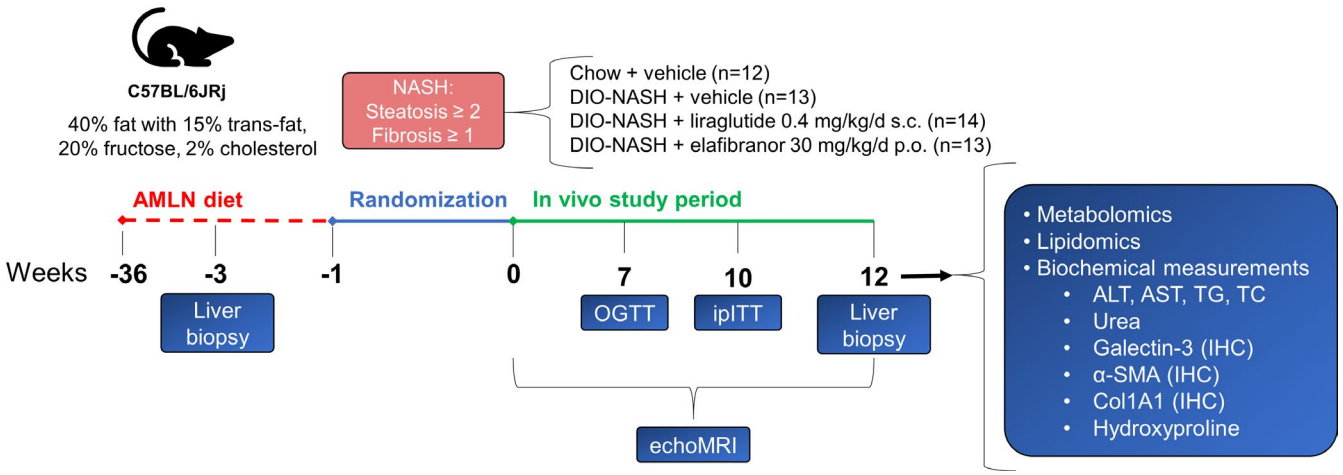

FIGURE 1 Schematic representation of study design. ALT, alanine aminotransferase; AST, aspartate aminotransferase; Col1a1, collagen 1a1; DIO, diet-induced obese; IHC, immunohistochemistry; ipITT, intraperitoneal insulin tolerance test; NASH, non-alcoholic steatohepatitis; OGTT, oral glucose tolerance test; TC, total cholesterol; TG, triglyceride; α-SMA, alpha-smooth muscle actin

TABLE 1 Metabolic outcomes of liraglutide and elafibranor treatment (Means ± SEM)

		Chow +vehicle	DIO-NASH + vehicle	DIO-NASH + liraglutide	DIO-NASH + elafibranor	*P*-ANOVA
Body weight (g)	Pre	30.2 ± 0.7***	38.5 ± 0.6	37.6 ± 0.7	36.9 ± 1.0	<0.001
	Post	30.3 ± 0.6***	40.1 ± 0.6	35.3 ± 0.5***	32.5 ± 1.0***†	<0.001
	Δ	0.1 ± 0.2	1.6 ± 0.5	−2.3 ± 0.5***	−4.4 ± 0.8***†	<0.001
	P	*0.570*	***0.012***	***<0.001***	***<0.001***	
Fat mass (g)	Pre	2.4 ± 0.2***	7.9 ± 0.5	6.8 ± 0.4	6.4 ± 0.5	<0.001
	Post	2.7 ± 0.2***	9.0 ± 0.5	4.9 ± 0.2***	3.7 ± 0.3***†	<0.001
	Δ	0.3 ± 0.2	1.0 ± 0.4	−1.9 ± 0.4***	−2.7 ± 0.5***	<0.001
	P	*0.100*	***0.028***	***<0.001***	***<0.001***	
Lean mass (g)	Pre	16.4 ± 0.5**	19.1 ± 0.2	18.7 ± 0.5	19.0 ± 0.6	0.001
	Post	16.8 ± 0.5**	19.2 ± 0.6	17.6 ± 0.4	17.0 ± 0.6*	0.010
	Δ	0.4 ± 0.5	0.1 ± 0.6	−1.0 ± 0.5	−1.9 ± 0.5*	0.018
	P	*0.420*	*0.900*	*0.077*	***0.005***	
Water mass (g)	Pre	0.1 ± 0.0	0.1 ± 0.0	0.2 ± 0.0	0.2 ± 0.0	0.149
	Post	0.2 ± 0.0	0.1 ± 0.0	0.2 ± 0.0	0.1 ± 0.0	0.239
	Δ	0.1 ± 0.0	0.0 ± 0.0	0.0 ± 0.1	−0.1 ± 0.1	0.075
	P	***0.009***	*0.299*	*0.851*	*0.153*	
4h-Fasting glucose (mmol/L)	Pre	7.5 ± 0.2*	8.2 ± 0.1	8.0 ± 0.2	7.6 ± 0.2*	0.010
	Post	7.8 ± 0.1	7.5 ± 0.2	6.7 ± 0.1**	6.4 ± 0.2***	<0.001
	Δ	0.3 ± 0.2*	−0.6 ± 0.2	−1.3 ± 0.2	−1.1 ± 0.2	<0.001
	P	*0.198*	***0.017***	***<0.001***	***<0.001***	
4h-Fasting insulin (pg/mL)	Pre	462.2 ± 64.8***	782.1 ± 64.8	644.3 ± 58.3	643.7 ± 33.5	0.004
	Post	371.8 ± 41.2***	689.9 ± 58.9	615.5 ± 74.0	297.2 ± 21.9***†††	<0.001
	Δ	−90.4 ± 91.8	−92.3 ± 75.7	−28.8 ± 91.1	−346.5 ± 33.9†	0.024
	P	*0.346*	*0.248*	*0.757*	***<0.001***	
Week 7-8 OGTT (mmol/l)	0	7.2 ± 0.2	7.3 ± 0.2	6.4 ± 0.1**	5.8 ± 0.2***	Trt<0.001 Tm<0.001 Tm*Trt<0.001
	15	13.1 ± 0.3	13.6 ± 0.4	14.2 ± 0.4	10.8 ± 0.4***†††	
	30	9.9 ± 0.4	10.7 ± 0.5	10.4 ± 0.5	8.3 ± 0.3**†	
	60	8.4 ± 0.2	8.5 ± 0.3	6.7 ± 0.2***	7.1 ± 0.2**	
	120	7.7 ± 0.2	7.7 ± 0.3	6.4 ± 0.2**	7.2 ± 0.2	
	180	7.1 ± 0.2	6.9 ± 0.2	5.9 ± 0.1*	6.9 ± 0.2†	
AUC		1528.0 ± 34.4	1550.0 ± 52.3	1355.0 ± 26.6**	1348.0 ± 32.1**	<0.001
Week 9-10 ipITT (mmol/l)	0	7.7 ± 0.1	7.8 ± 0.1	6.9 ± 0.2**	6.2 ± 0.2***	Trt<0.001 Tm<0.001 Tm*Trt<0.001
	15	5.3 ± 0.2***	6.6 ± 0.2	5.3 ± 0.2**	4.6 ± 0.2***	
	30	4.8 ± 0.1	5.1 ± 0.1	4.0 ± 0.1***	3.7 ± 0.1***	
	60	3.3 ± 0.2	3.6 ± 0.2	2.6 ± 0.2***	3.0 ± 0.2	
	120	4.4 ± 0.1	4.4 ± 0.3	3.8 ± 0.2	4.2 ± 0.3	
	180	5.6 ± 0.2	5.6 ± 0.2	5.4 ± 0.2	5.6 ± 0.3	
AUC		822.4 ± 12.7	868.0 ± 29.1	728.2 ± 18.0***	756.6 ± 34.1**	0.001

AUC, Area under the curve; ipITT, Intraperitoneal Insulin Tolerance Test; OGTT, Oral glucose tolerance test; *P*, *P*-value from paired *t*-test comparing values before (pre) and after (post) biopsy, bold when statistically significant; Δ, absolute difference (post-pre treatment score); ANOVA, for the horizontal comparison between different subject group; Trt, Time, Time*trt, P-values for factors treatment, time and time x treatment in the 2-way ANOVA respectively. Data are presented as means ± SEM.

*$P < .05$ compared with DIO-NASH + vehicle.; **$P < .01$ compared with DIO-NASH + vehicle.; ***$P < .001$ compared with DIO-NASH + vehicle.

†$P < .05$ for DIO-NASH + liraglutide compared with DIO-NASH + elafibranor in the Bonferroni tests.

††$P < .01$ for DIO-NASH + liraglutide compared with DIO-NASH + elafibranor in the Bonferroni tests.

†††$P < .001$ for DIO-NASH + liraglutide compared with DIO-NASH + elafibranor in the Bonferroni tests.

has been previously described in detail[6] and is also summarized in the Supporting Information.

2.7 | Statistics

Statistical analysis is described in detail in the Supporting Information and was performed with GraphPad Prism 8 (GraphPad Software Inc) and MetaboAnalystR.[31] Briefly, one- or two-way (for OGTT and ipITT) ANOVA with post-hoc Bonferroni tests for each group vs DIO-NASH + vehicle and for DIO-NASH + liraglutide vs DIO-NASH + elafibranor was performed for all parameters demonstrated in figures. Data are presented as means ± SEM. Sparse partial least squares-discriminant analysis (sPLS-DA), heatmaps with hierarchical clustering, significance analysis of microarrays (SAMa), random forest and pathway analysis using KEGG library was performed for the normalized concentrations of the lipidomic and/or metabolomic parameters (Supporting Information).

3 | RESULTS

3.1 | Liraglutide and elafibranor reduce body weight by decreasing mainly fat mass; they improve postprandial glucose levels and increase insulin sensitivity

Liraglutide and elafibranor led to significant body weight loss, especially the first two weeks of treatment (Figure S1). Energy intake was reduced the first 12 days of treatment with liraglutide but not later, whereas energy intake was not affected by elafibranor compared with vehicle (Figure S1). The body weight loss was mainly fat mass loss for liraglutide and both fat and muscle mass loss for elafibranor. No changes in water mass were observed. Glucose profiles assessed by OGTT and insulin sensitivity by ipITT were improved to a similar degree by both treatments (Table 1).

3.2 | Liraglutide and elafibranor improve blood lipid profile, transaminases and liver histology

Biochemical analysis showed lower levels of AST and ALT mainly in liraglutide-treated mice (Table 2). In addition, serum TC was lower in both treatments whereas serum TGs were only marginally affected, especially by elafibranor treatment (Table 2). Liver weight was reduced by liraglutide but increased with elafibranor compared with vehicle. Both treatments ameliorated liver histology, according to pre-to-post NAFLD activity score (NAS), and equally reduced lobular inflammation and hepatocellular ballooning, whereas elafibranor led to a slightly larger reduction of steatosis score compared with liraglutide and to a profound reduction of fibrosis stage (qualitative assessment based on collagen localization) compared to vehicle (Table 2, Figures S2 and S3).

3.3 | Elafibranor affects more robustly markers of hepatic lipid accumulation and liraglutide of Kupffer and hepatic stellate cell activation

Liver lipid content and TG were lower in both treatments compared with vehicle (Table 2), but more profoundly in elafibranor, thus suggesting a stronger impact of elafibranor on hepatic lipid accumulation and metabolism compared with liraglutide. Similarly, hydroxyproline levels, which are a quantitative marker of collagen synthesis and degradation and indirectly of liver fibrosis, were low in both treatments, but lower with elafibranor compared with liraglutide. In contrast, liraglutide treatment led to lower percentage of Galectin-3, α-SMA and Col1a1 positive areas in liver IHC compared both with vehicle and elafibranor (Table 2 and Figure S4). Galectin-3 is a reliable marker of Kupffer and hepatic stellate cell activation[28]; α-SMA is also an established marker of differentiation of hepatic stellate cells to fast proliferative collagen producing myofibroblast-like cells.[29] Finally, Col1a1 is one of the main components of type I collagen and is also a marker of liver fibrosis. Thus, the lower percentage of positive areas for all three above parameters suggest less activation of Kupffer and hepatic stellate cells to produce collagen after 12 weeks of treatment with liraglutide.[32]

3.4 | Liraglutide and elafibranor significantly but differentially affect hepatic lipidome

In order to assess the effects of both treatments on hepatic lipid composition a lipidomic mass spectrometric analysis was performed which identified 1001 lipids. sPLS-DA (Figure 2A) demonstrated that DIO-NASH + vehicle mice form a separate cluster from lean chow + vehicle mice, indicating profound differences in hepatic lipidome between the two groups. DIO-NASH + liraglutide mice partially separate from the DIO-NASH + vehicle group, suggesting a partial restoration of lipidomic profile, whereas DIO-NASH + elafibranor mice form a distinct cluster, indicating extensive effects of the treatment on lipidome. According to SAMa, 468 parameters were significantly different among the four groups (Figure 2B). Hierarchical clustering of the 100 most significantly different lipids (Figure 2C) and random forest classification analysis (Figure 2D) could distinguish treatment groups with very high accuracy (~92% in random forest) using mostly triacylglycerol (TAG) species (Figure 2E).

3.5 | Elafibranor has a more profound effect compared with liraglutide on the concentrations and composition of hepatic lipids

When investigating the lipid groups, AMLN diet led to a significant increase of TAG, diacylglycerol (DAG), and cholesterol ester (CE)

TABLE 2 Biochemical and hepatic outcomes of liraglutide and elafibranor treatment (means ± SEM)

	Chow + vehicle	DIO-NASH + vehicle	DIO-NASH + liraglutide	DIO-NASH + elafibranor	*P* ANOVA
Blood parameters					
AST (U/L)	50.9 ± 1.2***	233.7 ± 30.1	97.2 ± 9.9***	205.1 ± 30.5††	<.001
ALT (U/L)	30.1 ± 0.7***	221.6 ± 36.4	47.8 ± 7.5***	143.6 ± 27.5††	<.001
TC (mmol/L)	2.7 ± 0.1***	8.0 ± 0.3	5.0 ± 0.3***	5.7 ± 0.2***	<.001
TG (mmol/L)	1.4 ± 0.1***	0.9 ± 0.1	0.6 ± 0.0	0.5 ± 0.1*	<.001
Urea (mmol/L)	8.7 ± 0.3*	7.5 ± 0.1	7.9 ± 0.3	8.0 ± 0.4	.053
Histology (scores)					
NAS					
Pre	0.1 ± 0.1***	4.9 ± 0.1	5.4 ± 0.2	5.6 ± 0.2**	<.001
Post	0.0 ± 0.0***	5.1 ± 0.1	4.0 ± 0.2***	3.6 ± 0.2***	<.001
Δ	−0.1 ± 0.1	0.2 ± 0.2	−1.4 ± 0.3***	−2.0 ± 0.2***	<.001
P	.339	.436	**<.001**	**<.001**	
Steatosis					
Pre	0.1 ± 0.1***	3.0 ± 0.0	3.0 ± 0.0	3.0 ± 0.0	<.001
Post	0.0 ± 0.0***	3.0 ± 0.0	2.6 ± 0.1*	2.1 ± 0.1***†††	<.001
Δ	−0.1 ± 0.1	0.0 ± 0.0	−0.4 ± 0.1	−0.9 ± 0.1***††	<.001
P	.339	NA	**.019**	**<.001**	
Lobular inflammation					
Pre	0.0 ± 0.0***	1.9 ± 0.1	2.1 ± 0.1	2.4 ± 0.2*	<.001
Post	0.0 ± 0.0***	1.8 ± 0.1	1.4 ± 0.2*	1.5 ± 0.1	<.001
Δ	0.0 ± 0.0	−0.1 ± 0.1	−0.7 ± 0.2**	−0.8 ± 0.2**	<.001
P	NA	.585	**.003**	**<.001**	
Hepatocyte Ballooning					
Pre	0.0 ± 0.0	0.0 ± 0.0	0.3 ± 0.1	0.2 ± 0.1	.045
Post	0.0 ± 0.0*	0.2 ± 0.1	0.0 ± 0.0*	0.0 ± 0.0*	.020
Δ	0.0 ± 0.0	0.2 ± 0.1	−0.3 ± 0.1**	−0.2 ± 0.1*	.006
P	NA	.082	**.040**	.082	
Fibrosis stage					
Pre	0.0 ± 0.0***	2.2 ± 0.2	2.1 ± 0.1	2.2 ± 0.1	<.001
Post	0.0 ± 0.0***	2.1 ± 0.2	1.9 ± 0.1	1.7 ± 0.1	<.001
Δ	0.0 ± 0.0	−0.2 ± 0.1	−0.2 ± 0.1	−0.5 ± 0.1*	.009
P	NA	.165	.082	**.003**	
Liver parameters					
Weight (g)	1.4 ± 0.1***	3.4 ± 0.1	2.0 ± 0.1***	4.2 ± 0.3**†††	<.001
Lipid content (%area)	1.1 ± 0.1***	26.0 ± 1.7	13.1 ± 1.0***	7.2 ± 1.1***††	<.001
TG (mg/g liver)	9.4 ± 0.5***	89.1 ± 11.2	57.0 ± 4.7**	45.2 ± 4.9***	<.001
TC (mg/g liver)	4.0 ± 0.1***	10.5 ± 0.9	8.7 ± 0.6	8.9 ± 0.4	<.001
HP (ug/g liver)	19.3 ± 1.0***	87.3 ± 8.1	63.0 ± 6.7*	38.9 ± 3.9***†	<.001
Markers of Kupffer and hepatic stellate cell activation					
Col1a1 (% area)	1.8 ± 0.1***	8.0 ± 0.9	5.5 ± 0.6*	6.3 ± 0.5	<.001
α-SMA (% area)	0.5 ± 0.0***	3.7 ± 0.3	1.5 ± 0.1***	2.6 ± 0.3***††	<.001
Galectin-3 (% area)	0.6 ± 0.0***	3.2 ± 0.2	1.7 ± 0.1***	2.4 ± 0.2**††	<.001

Note: For histology, NAS score graded 0-8; steatosis, 0-3; inflammation, 0-2; ballooning, 0-2; fibrosis stage, 0-4. *P*, *P* value from paired *t* test comparing values before (pre) and after (post) biopsy, bold when statistically significant; Δ, absolute difference (post-treatment − pre-treatment score); ANOVA, for the horizontal comparison between different subject group. Data are presented as means ± SEM.

Abbreviations: ALT, alanine transaminase; AST, aspartate transaminase; ColIA1, Collagen type I Alpha-1; HP, hydroxyproline; NA, not applicable; NAS, NAFLD activity score; TC, total cholesterol; TG, triglycerides; α-SMA, alpha-smooth muscle actin.

*$P < .05$ compared with DIO-NASH + vehicle.

**$P < .01$ compared with DIO-NASH + vehicle.

***$P < .001$ compared with DIO-NASH + vehicle.

†$P < .05$ for DIO-NASH + liraglutide compared with DIO-NASH + elafibranor in the Bonferroni tests.

††$P < .01$ for DIO-NASH + liraglutide compared with DIO-NASH + elafibranor in the Bonferroni tests.

†††$P < .001$ for DIO-NASH + liraglutide compared with DIO-NASH + elafibranor in the Bonferroni tests.

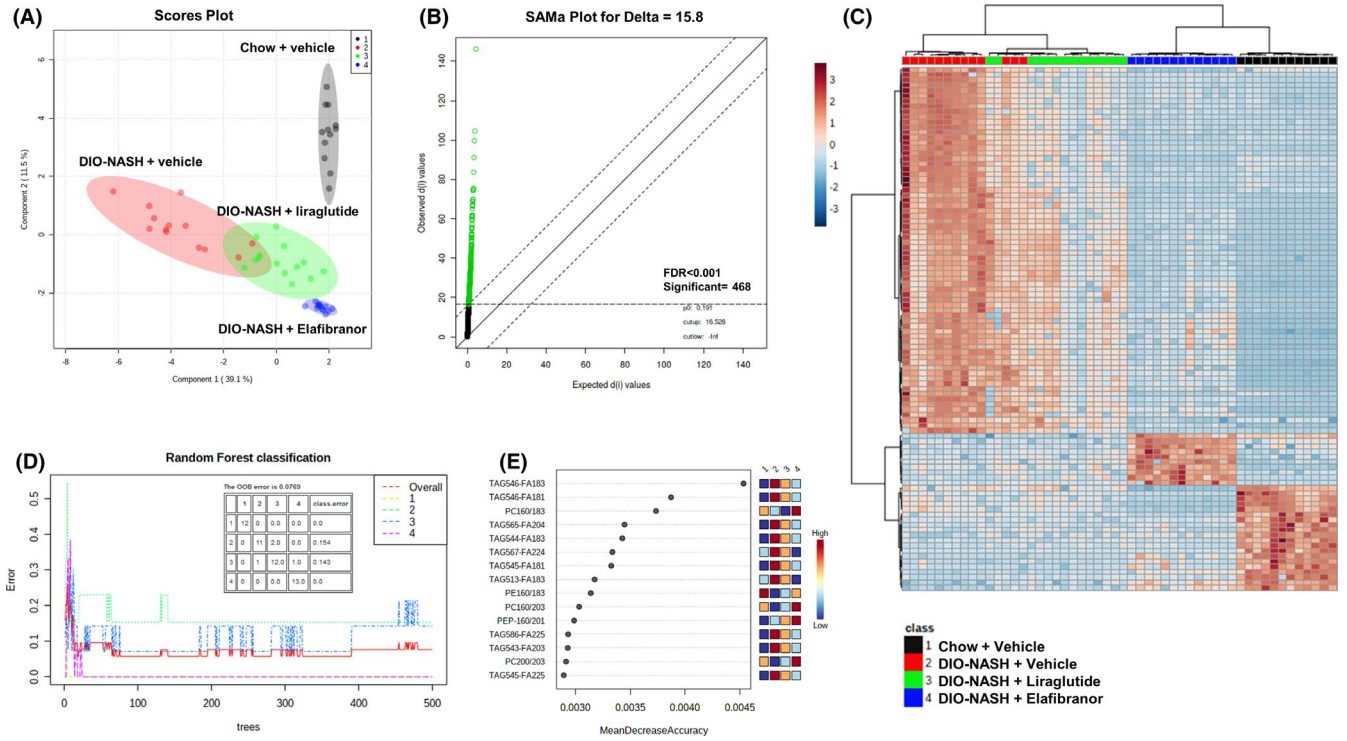

FIGURE 2 Effects of liraglutide and elafibranor on hepatic lipidome. (A) Score plot of the two main principal components of sparse partial least squares discriminant analysis (sPLS-DA) for the four treatment groups (each dot corresponds to one mouse and coloured circles to 95% confidence intervals); (B) significance analysis of microarrays (SAMa) identifies 468 parameters that are significantly different between groups (green dots); (C) heatmap with hierarchical clustering of the 100 most significantly different parameters among groups; (D) random forest classification with up to 500 decision trees; (E) most important parameters and their level of contribution for random forest classification. Groups 1: chow + vehicle; 2: DIO-NASH + vehicle; 3: DIO-NASH + liraglutide; 4: DIO-NASH + elafibranor. DIO, diet-induced-obese; FDR, false discovery rate; NASH, non-alcoholic steatohepatitis; OOB, out-of-bag error

species (Figure 3A) and to a reduction of phospholipids (Figure 3B) and sphingolipids (Figure 3C), which is in absolute agreement with the lipid changes observed in advanced human NAFLD.[24,32] Treatment with liraglutide and elafibranor partially restored the changes in glycerides (TAG, DAG, monoacylglycerols [MAGs]), CE, and phospholipids (phosphatidylcholines [PC], phosphatidylethanolamines [PE], PC/PE ratio), with the improvement being more profound with elafibranor than with liraglutide (Figure 3A,B). Liraglutide treatment did not affect sphingolipids, whereas elafibranor had a modest impact by increasing the concentrations of hexosyl-ceramides and decreasing the concentrations of lactosyl-ceramides and sphingomyelins (Figure 3C). The reduction in TAG with elafibranor was more profound in species with a high number of double bonds (increasing unsaturation), whereas the increase in PC and PE was exclusively observed in species with a low number of double bonds (Figure 3E). These patterns may be related to the higher instability of the highly unsaturated species, which facilitates their oxidation. This is further supported by the increased concentration of 3-hydroxybutyrate with elafibranor treatment, which is a ketone body deriving from the main product of β-oxidation, that is, acetyl-CoA (Figure 3D). Concentrations of carnitines and acyl-carnitines, which are responsible for the transport of fatty acids (FAs) from cytosol or peroxisome to mitochondria for β-oxidation, were higher in both treatment groups compared with DIO-NASH + vehicle (Figure 3D). However, the effect of liraglutide on carnitines was more selective, in contrast to elafibranor treatment, which additionally increased the concentrations of carnitines that are associated with higher cellular apoptosis (palmitoylcarnitine), FA synthesis and impaired FA oxidation (malonylcarnitine) (Figure 3D).

Liraglutide treatment did not affect the metabolic pathways of the most important ω-3 (linolenate) and ω-6 (linoleate) fatty acids (Figure 4A,B). In contrast, elafibranor led to higher levels of eicosapentaenoic acid (EPA). Both downstream and upstream of EPA and lower concentrations of the relevant lipids were observed, suggesting that elafibranor may facilitate the accumulation of the anti-inflammatory EPA. Elafibranor led also to a reduction of linoleate and its metabolites (ie, hydroxyoctadecadienoic acids [HODEs] and dihydroxyoctadecenoic acids [DiHOMEs]) that are related to oxidative stress and inflammation (Figure 4B,C). Importantly, elafibranor reduced also the concentrations of arachidonate, resulting also in lower concentrations of metabolites involved in prostaglandin (PG) synthesis (PGF2α and 6-ketoPGF1α) and hence in inflammation (Figure 4B,C).

3.6 | Liraglutide and elafibranor significantly affect hepatic metabolome

A metabolomics analysis identified 579 known metabolites. sPLS-DA analysis of the three main components formulated four distinct

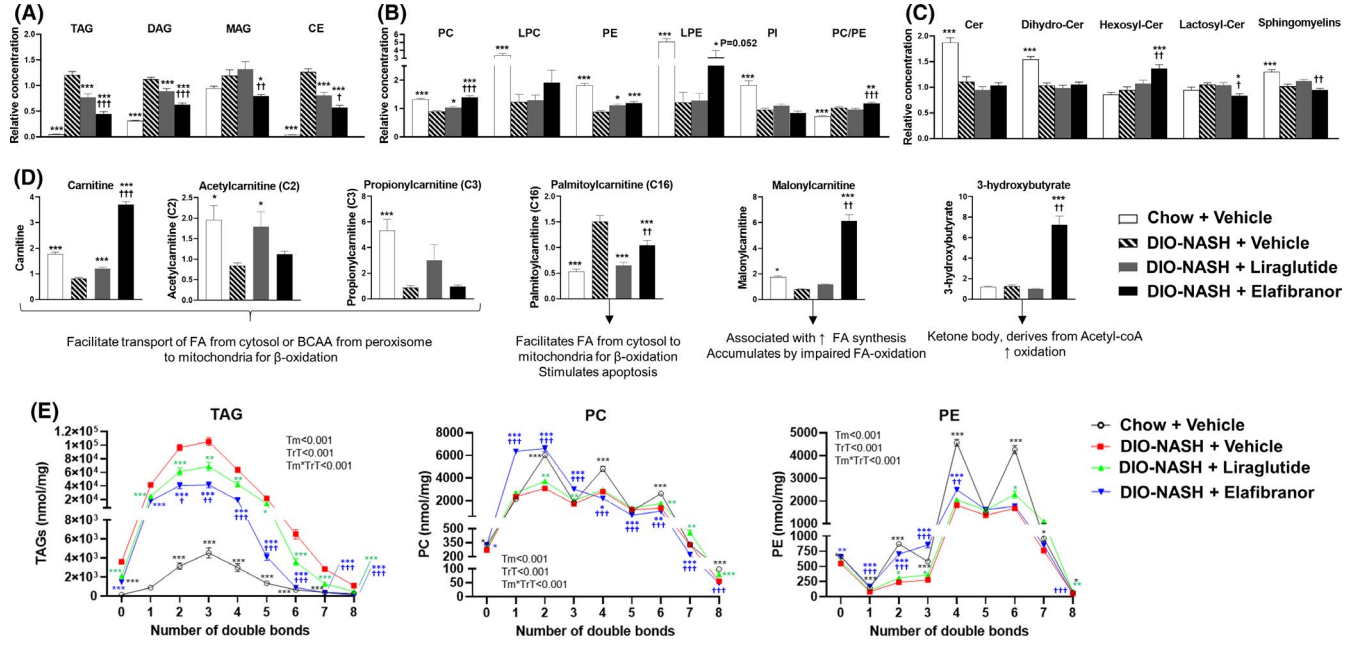

FIGURE 3 Effects of liraglutide and elafibranor on hepatic lipid classes and composition. Relative concentrations in the liver of (A) glycerides, (B) phospholipids, (C) sphingolipids and (D) carnitines. (E) Further analysis of hepatic concentrations of TAG, PC and PE based on the number of double bonds. *,**,*** and †, ††, ††† indicate $P < .05, .01, .001$ for each group vs NASH treated with vehicle (stars) and for liraglutide vs elafibranor (crosses), respectively (Bonferroni post-hoc *t* tests performed by *P* ANOVA < .001). CE, cholesterol ester; DAG, diacylglycerol; DIO, diet-induced-obese; MAG, monoacylglycerol; NASH, non-alcoholic steatohepatitis; PC, phosphatidylcholine; PE, phosphatidylethanolamines; TAG, triacylglycerol

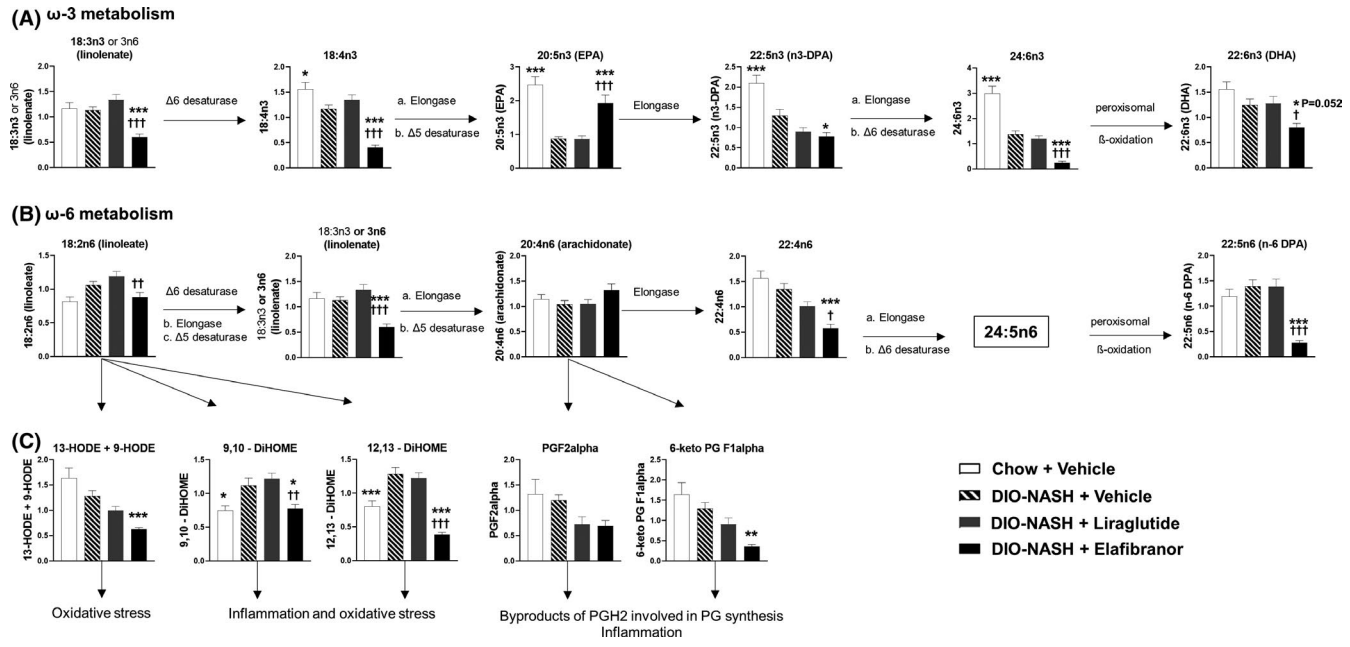

FIGURE 4 Effects of liraglutide and elafibranor on the metabolism of ω-3 and ω-6 pathway. (A) Metabolic pathway of linolenate, (B) metabolic pathway of linoleate, (C) metabolic products of the metabolism of linoleate and arachidonate. *, **, *** and †, ††, ††† indicate $P < .05, .01, .001$ for each group vs DIO-NASH treated with vehicle (stars) and for liraglutide vs elafibranor (crosses), respectively (Bonferroni post-hoc *t* tests performed by *P* ANOVA < .001). DIO, diet-induced-obese; NASH, non-alcoholic steatohepatitis

clusters, one for each group, thus suggesting robust differences between DIO-NASH + vehicle and chow + vehicle as well as between treatments in hepatic metabolome (Figure S5A). SAMa identified 141 significantly different parameters between groups (Figure S5B). Hierarchical clustering of the 100 most significantly different metabolites (Figure S5C) and random forest classification

analysis (Figure S5D) could distinguish treatment groups with very high accuracy (~96% in random forest). Pathway analysis identified several metabolic processes that may be affected by liraglutide or elafibranor, which were mainly related to carbohydrate and amino acid metabolism (Figure S5E,F).

3.7 | Elafibranor may regulate oxidative stress and fatty acid metabolism by affecting methionine, glutathione and pantothenate-CoA metabolism

Elafibranor treatment was associated with a significant improvement of methionine metabolism, characterized by increased concentrations of several intermediates (S-adenosylmethionine [SAM], S-adenosylhomocysteine (SAH) and cystathionine), as well as of contributors to its metabolism (betaine, 5-methyltetrahydrofolate [5-MeTHF]) (Figure 5A). The accumulation of SAM encourages the production of α-ketobutyrate (not measured in our study) and cysteine which was increased approximately four-fold in the elafibranor group (Figure 5A). Cysteine participates in glutathione metabolism, and indeed, a significant increase in glutathione (GSH) was observed in the elafibranor group, which was also accompanied by robust increases of metabolites with antioxidant properties (ie, S-lactoylglutathione) and of markers of lipid peroxidation (ie, glutathione-4-hydroxynonenal, GSHNE) (Figure 5B). Additionally, cysteine may affect pantothenate and CoA metabolism. Indeed, this pathway was robustly stimulated, leading to very high hepatic CoA levels (Figure 5C). The increased CoA can be either used for energy production through the tricarboxylic acid cycle (TCA) cycle or for fatty acid metabolism, that is, fatty acid synthesis or oxidation. No robust and consistent changes in TCA cycle metabolite concentrations were observed (Figure S6).

3.8 | Liraglutide and elafibranor differentially affect bile acid and carbohydrate metabolism

DIO-NASH + vehicle mice demonstrated a reduction in the concentrations of both the primary and secondary bile acids and their metabolites compared with chow + vehicle mice (Figure 6A,B). Treatment with elafibranor further reduced the concentrations of bile acids whereas, in contrast, liraglutide significantly increased the concentrations especially of secondary bile acids. Liraglutide and elafibranor also demonstrated differential effects on hepatic carbohydrate metabolism (Figure 6C). Specifically, liraglutide restored the concentrations of metabolites related to pentose synthesis through the pentose-phosphate pathway as well as the concentrations of metabolites related to glycogen synthesis and degradation (Figure 6C). Elafibranor increased the hepatic concentrations of metabolites involved in glycolysis, in the hexosamine pathway, and in the formation of uridine diphosphate (UDP)-glucose (Figure 6C). These changes

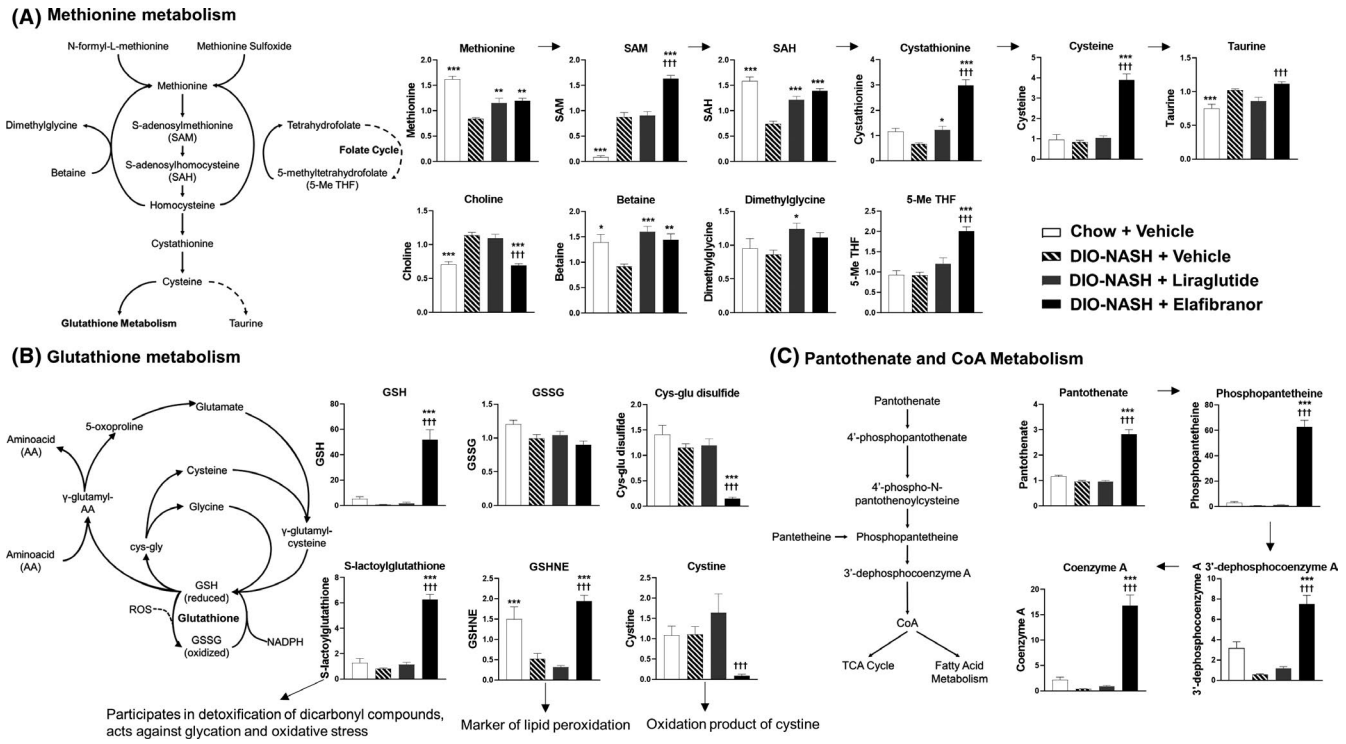

FIGURE 5 Effects of liraglutide and elafibranor on (A) methionine, (B) glutathione and (C) pantothenate and CoA metabolism. *, **, *** and †, ††, ††† indicate $P < .05, .01, .001$ for each group vs DIO-NASH treated with vehicle (stars) and for liraglutide vs elafibranor (crosses), respectively (Bonferroni post-hoc *t* tests performed by *P* ANOVA < .001). DIO, diet-induced-obese; NASH, non-alcoholic steatohepatitis; TCA, tricarboxylic acid

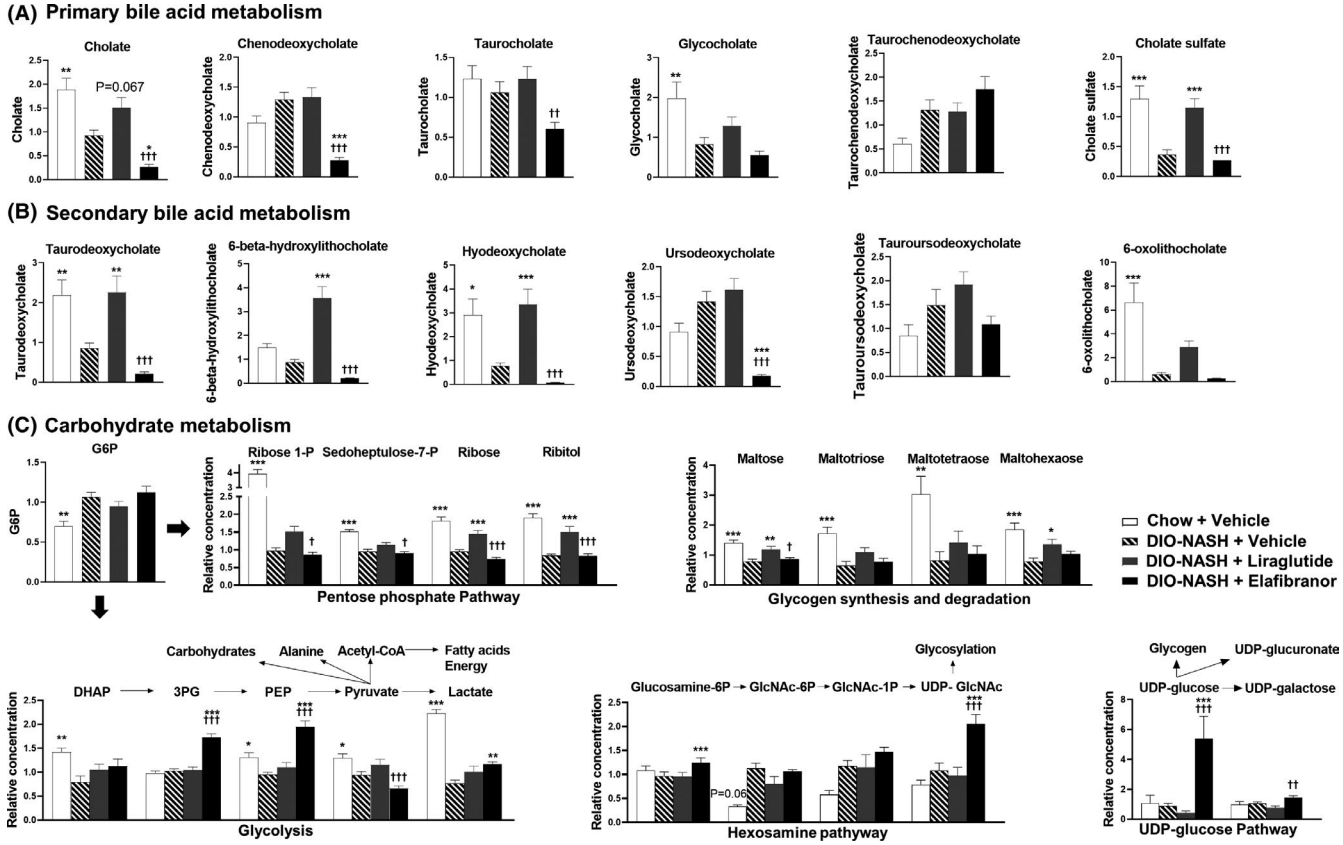

FIGURE 6 Effects of liraglutide and elafibranor on (A) primary bile acid metabolism, (B) secondary bile acid metabolism, (C) carbohydrate metabolism (G6P, pentose phosphate pathway, glycogen synthesis and degradation, glycolysis, hexosamine pathway, UDP-glucose pathway), *, **, *** and †, ††, ††† indicate $P < .05$, .01, .001 for each group vs DIO-NASH treated with vehicle (stars) and for liraglutide vs elafibranor (crosses), respectively (Bonferroni post-hoc *t* tests performed by *P* ANOVA < .001). DIO, diet-induced-obese; NASH, non-alcoholic steatohepatitis; UDP, uridine diphosphate

indicate that liraglutide treatment guides glucose metabolism to increased formation of pentoses that facilitate nucleic acid formation as well as to high glycogen utilization turnover, whereas elafibranor uses glucose for enhancing fatty acid metabolism, glycosylation, and possibly glycogen formation. Finally, DIO-NASH + vehicle mice had approximately 50% lower hepatic concentrations in all amino acids compared with chow + vehicle mice (Figure S7). DIO-NASH mice treated with liraglutide or with elafibranor had still lower concentrations in amino acids compared with chow + vehicle, but significantly higher compared with DIO-NASH + vehicle mice, which indicates a partial restoration of hepatic amino acid levels with the two treatments (Figure S7).

4 | DISCUSSION

We first confirm herein elafibranor and liraglutide actions to improve NASH significantly in an established biopsy-confirmed mouse model of advanced NASH with fibrosis. Importantly, we demonstrate that elafibranor and liraglutide affect robustly but differentially hepatic lipidome and metabolome as well as Kupffer and hepatic stellate cell activation. Elafibranor mainly restores hepatic lipid profile and regulates pathways related to fatty acid β-oxidation, inflammation and oxidative stress. Liraglutide mainly reduces the activation of Kupffer and hepatic stellate cells, and it has a modest fine-tuning role on hepatic lipidome compared with elafibranor. Liraglutide has also more profound effects on carbohydrate metabolism by utilizing excess glucose for the formation of facilitators of nucleic acid synthesis and by enhancing glycogen utilization-turnover. These actions provide the basis for potential synergistic effects.

The reduction in TAG, DAG and MAG observed with elafibranor treatment is in agreement with the histological improvement in steatosis observed in our study, in other murine NASH models and human clinical trials.[10,15,20] A stimulation of β-oxidation due to an upregulation of genes involved in peroxisomal and mitochondrial β-oxidation has been proposed as the main mechanism of hepatic lipid reduction.[6] Herein, we show that both the concentrations of CoA that reacts with fatty acids to form acyl-CoAs to be used for β-oxidation, as well as the concentrations of acylcarnitines, that facilitate the transport of the acyl-CoAs from the cytosol to mitochondria for β-oxidation, are increased with elafibranor. Thus β-oxidation, especially of the more unsaturated and thus more unstable TGs is upregulated by elafibranor. In agreement with the above, we see an almost six-fold increase in 3-hydroxybutyrate, which is a ketone body deriving from end-products of β-oxidation. In contrast, we see minor changes in concentrations of TCA cycle products. Thus,

elafibranor treatment leads to increased fatty β-oxidation resulting though in almost exclusively increased ketone body formation and not in higher direct release of energy through the TCA cycle in the liver. Additionally, elafibranor increased the PC/PE ratio. A low ratio is observed both in our mouse model and in humans with NAFLD[32] and is associated with lipid droplet instability that leads to breaking and consolidation of lipids in larger droplets.[24,33] Additionally, PC deficiency leads to unstable very low-density lipoprotein (VLDL) particles that are not secreted by the liver but are partially intracellularly degraded leading to increased hepatic lipid accumulation.[24,33] Hence, the increase in PC and PC/PE ratio with elafibranor may further improve lipid metabolism by reducing large lipid droplet formation, in agreement with our findings in liver histology, and probably by restoring hepatic lipid clearance through VLDL secretion.

The anti-inflammatory and anti-apoptotic functions of elafibranor may also be related to the improvement in hepatic lipid metabolism. Specifically, in our study, elafibranor reduced the hepatic levels of saturated TG. Saturated FAs induce inflammation by activating NF-κB and inflammasomes and thus leading to increased secretion of pro-inflammatory cytokines and chemotaxis.[24] Additionally, they promote endoplasmic reticulum stress and induce caspases, hence promoting hepatocyte apoptosis.[24] Treatment with elafibranor also stimulated methionine and glutathione metabolism, which led to elevated GSH and S-lactoylglutathione. GSH is a major scavenger of reactive oxygen species whereas S-lactoylglutathione participates in detoxification from dicarbonyl compounds, acting against glycation and oxidative stress.[34] Elafibranor additionally reduced metabolites of linoleate that are positively associated with NAFLD severity and constitute reliable markers of oxidative stress (eg, 13-HODE, 9-HODE),[35] or may increase neutrophil chemoattractant activity (9,10-DiHOME and 12,13-DiHOME).[36] Elafibranor increased the concentrations of EPA that drives the formation of several specialized pro-resolving mediators (SPMs), such as resolvins, protectins, maresins and lipoxins, which lead to inflammatory resolution.[24] Additionally, it decreased the levels of arachidonate metabolites, such as the PGF2alpha prostaglandin and the 6-keto PG F1alpha, metabolite of prostacyclin, that both have a clear pro-inflammatory role.[24] Altogether, the robust effect of elafibranor on hepatic lipidome probably contributes, through the above mechanisms, to the observed reduction in hepatic inflammation and oxidative stress.

Liraglutide has demonstrated anti-steatotic and anti-inflammatory effects in different mouse models of NAFLD[8,9,11-13] as well as in human clinical trials.[14,16-19,21] Several studies have suggested that liraglutide improves hepatic lipid deposition, endoplasmic reticulum stress and oxidative stress by activating autophagy.[8,9,12] Additionally, it increases hepatic insulin sensitivity and reduces hepatic de novo lipogenesis.[37] Given that the presence of GLP-1 receptors in the liver is still debated, the effects of liraglutide may be indirect through the systemic improvement of insulin sensitivity, suppression of adipose tissue lipolysis and reduction of energy intake leading to weight loss[37] and through upregulation of adiponectin.[38] Here we show that, in contrast to elafibranor, liraglutide has modest effects on hepatic lipid composition. It reduces TAGs and DAGs and increases PC, PE and acyl-carnitines but to a much lesser extent compared with elafibranor.

Although the improvement in hepatic inflammation in liver histology is similar between liraglutide and elafibranor, liraglutide has no major impact on the hepatic levels of lipid metabolites that are related to oxidative stress, β-oxidation, or of precursors of pro- or anti-inflammatory molecules. Thus, the anti-inflammatory properties of liraglutide should probably and at least partially be attributed to other mechanisms than the improvement of hepatic lipid profile. For example, it has been shown that liraglutide can modulate Kupffer cell polarization to increase the anti-inflammatory M2 phenotype.[39] In agreement with the above, we observe lower levels of Galectin-3 and α-SMA in DIO-NASH + liraglutide mice compared with DIO-NASH + vehicle or DIO-NASH + elafibranor. Galectin-3 is expressed in bile duct epithelia and Kupffer cells in healthy conditions. During inflammation, it is additionally highly expressed in activated Kupffer cells and recruited macrophages and it is also co-expressed with α-SMA in hepatic stellate cells undergoing transformation to fibroblasts.[28] Thus, we show that liraglutide affects more robustly non-parenchymal cell function and specifically Kupffer and hepatic stellate cell activation, which explains its anti-inflammatory and anti-fibrotic effects in the liver.

Finally, we observe important differences between the effects of elafibranor and liraglutide on carbohydrate and bile acid metabolism. Specifically, liraglutide partially restored the levels of ribose (and its metabolites such as ribitol) in the liver. Ribose is an important pentose for nucleic acid synthesis and is additionally involved in multiple signalling pathways. Additionally, liraglutide partially restores the levels of intermediates of hepatic glycogen synthesis and degradation, thus contributing to the normalization of glycogen metabolism. Elafibranor had no effect on the above mechanisms but increased end-products of anaerobic glycolysis. Although the hexosamine and UDP-glucose pathways were not altered in DIO-NASH mice compared with healthy controls, elafibranor robustly increased the levels of end-products of these pathways, such as UDP-GlcNAc and UDP-glucose. These indicate possible effects of elafibranor on mechanisms of protein glycosylation and glycogen formation, whose impact on disease progression should be further evaluated in future studies. Furthermore, DIO-NASH mice demonstrated lower levels of several primary and secondary bile acids compared with healthy animals. Liraglutide treatment partially restored the levels of some of the bile acids, whereas elafibranor further decreased the concentrations in most of them. Many studies have shown that impaired bile acid metabolism is causally related to NAFLD and metabolic disbalance.[40] However, both lower and higher hepatic levels of bile acids have been reported in humans with NAFLD, with both beneficial and detrimental effects on metabolic outcomes depending on the site of action.[41,42] Whether liraglutide or elafibranor can be combined with medications that target bile acid metabolism, such as the Farnesoid X receptor agonist obeticholic acid,[40,43] should be addressed in future studies.

A finding in our study is the lower concentration of hepatic amino acids in mice on AMLN diet. Both liraglutide and elafibranor

treatment partially restored amino acid levels. The concentrations of circulating and hepatic branched-chain amino acids (BCAAs) have been associated positively with metabolic diseases, such as obesity, type 2 diabetes and NAFLD/NASH, but negatively with liver cirrhosis in observational studies in humans.[44] Additionally, supplementation of BCAAs exerts beneficial effects on metabolic and liver parameters in mice[45] and to a lesser extent in humans.[44,46] Whether the partial restoration of amino acid levels with both medications contributes to their beneficial hepatic effects or reflects compensatory changes in response to other actions of these medications remains to be investigated by future studies.

Clinical trials have shown initially that elafibranor increases hepatic insulin sensitivity, reduces plasma lipids and improves liver enzymes in obese patients,[20] and may induce resolution of NASH without worsening of fibrosis when used at high doses and in a specific pool of patients with advanced disease.[15] However, an interim analysis from a Phase 3 clinical trial reported no superiority for elafibranor compared with placebo.[47] Hence, it seems that there is limited translation of the very robust effects of elafibranor in rodent models of NAFLD to humans. This may be related to hyperresponsiveness of rodents in PPARα/δ agonism, indicated by the weight-reducing effects and hepatomegaly after treatment with elafibranor observed in mice but not in humans.[11,15] As we show in our study, elafibranor does not affect energy intake, thus the weight-reducing effects of elafibranor in mice are probably achieved by an increase in energy expenditure. In humans, PPARα/δ agonism has no reported effects on energy expenditure and consequently no effect on body weight. Similarly, the hepatomegaly in rodents treated with elafibranor has been attributed to peroxisome and hepatocyte proliferation due to hyperresponsiveness in PPARα agonism,[11,15] which is not observed in humans. The translational potential of the mouse findings has been questioned for most of the drug candidates for NAFLD treatment. GLP-1RA, liraglutide (1.8 mg for 48 weeks) led to resolution of NASH in significantly more subjects (39%) compared with placebo (9%) in a Phase 2 randomized clinical trial (RCT).[21] Semaglutide, a longer active alternative to liraglutide, in high doses and after longer treatment period (72 weeks) achieved more significant results with a resolution of NASH without worsening of fibrosis in 59% of subjects compared with 17% in the placebo group in a recently published Phase 2 RCT.[48] Weight loss that leads to improvement of insulin sensitivity and normalization of glucose homeostasis is considered a major contributor to the beneficial effects of these medications in the liver.[49,50] In our study, liraglutide led to significant weight loss in the first weeks of treatment, which was maintained throughout the study. These effects are similar to the weight-loss effects observed in humans at this dose (our dose corresponded to ~1.8 mg/day in humans).[49] Liraglutide at higher dose (3 mg/dL) or semaglutide can achieve even greater weight loss (up to 15%) in adults with overweight or obesity.[49,50] Given the complexity in the pathophysiology of NAFLD and the lack of improvement in liver status in many patients with NASH even with the most promising drugs, it seems necessary to combine medications in order to achieve a very effective treatment. In future studies, we expect that GLP-1RA analogs, notably semaglutide, which has recently received breakthrough status by the FDA for clinical trials in humans, to demonstrate, either alone in Phase 3 clinical trials or in combination regimens, similar in nature but apparently stronger metabolic effects than the ones observed with liraglutide.

Our study has several strengths and limitations. A strength of the study is the use of an established mouse model that develops not only hepatic steatosis but also inflammation and fibrosis and thus resembles the human course of NAFLD. Another strength is the performance of a liver biopsy before treatment initiation which enabled us to perform comparative evaluations of the post- vs pre-treatment liver status in histology. A limitation of the study is the lack of information about energy expenditure. Additionally, mice treated with elafibranor had a slightly higher NAS compared with mice treated with vehicle before treatment initiation. This may have led to an underestimation of the effects of elafibranor for the parameters that have been assessed only at treatment completion.

In conclusion, our study shows important differences in the regulation of hepatic lipidome, metabolome and Kupffer-hepatic stellate cells activation by elafibranor and liraglutide, which suggests different and rather complementary mechanisms of function and raises expectations for additive effects if both medications are used together or if they are combined with other treatments. Such approaches may overcome obvious limitations related to the suboptimal translation of results from animal studies in humans in almost all medications targeting NAFLD and thus deserve further evaluation in future studies.

CONFLICT OF INTEREST

M. F. and S. S. V. own stocks in and are employed by Gubra. C. S. M. owns stocks in Coherus; has consulted for Coherus, Novo Nordisk, Amgen, Regeneron, Intercept and Genfit; and has received grants through his Institution BIDMC from Coherus and Novo Nordisk. No other potential conflicts of interest relevant to this article were reported.

ETHICS APPROVAL

All animal experiments were conducted in accordance with Gubra bioethical guidelines, which are fully compliant with internationally accepted principles for the care and use of laboratory animals.

DATA AVAILABILITY STATEMENT

Datasets are available from NiP upon reasonable request.

ORCID

Christos S. Mantzoros https://orcid.org/0000-0003-3755-8158

REFERENCES

1. Kechagias S, Nasr P, Blomdahl J, Ekstedt M. Established and emerging factors affecting the progression of nonalcoholic fatty liver disease. *Metabolism*. 2020;111:154183.
2. Polyzos SA, Kang ES, Boutari C, Rhee EJ, Mantzoros CS. Current and emerging pharmacological options for the treatment of nonalcoholic steatohepatitis. *Metabolism*. 2020;111:154203.

3. Polyzos SA, Perakakis N, Mantzoros CS. Fatty liver in lipodystrophy: a review with a focus on therapeutic perspectives of adiponectin and/or leptin replacement. *Metabolism*. 2019;96:66-82.
4. Pilitsi E, Farr OM, Polyzos SA, et al. Pharmacotherapy of obesity: available medications and drugs under investigation. *Metabolism*. 2019;92:170-192.
5. Upadhyay J, Polyzos SA, Perakakis N, et al. Pharmacotherapy of type 2 diabetes: an update. *Metabolism*. 2018;78:13-42.
6. Perakakis N, Joshi A, Peradze N, et al. The selective peroxisome proliferator-activated receptor gamma modulator CHS-131 improves liver histopathology and metabolism in a mouse model of obesity and nonalcoholic steatohepatitis. *Hepatol Commun*. 2020;4(9):1302-1315.
7. Polyzos SA, Kountouras J, Mantzoros CS. Obesity and nonalcoholic fatty liver disease: from pathophysiology to therapeutics. *Metabolism*. 2019;92:82-97.
8. He Q, Sha S, Sun L, Zhang J, Dong M. GLP-1 analogue improves hepatic lipid accumulation by inducing autophagy via AMPK/mTOR pathway. *Biochem Biophys Res Commun*. 2016;476(4):196-203.
9. Sharma S, Mells JE, Fu PP, Saxena NK, Anania FA. GLP-1 analogs reduce hepatocyte steatosis and improve survival by enhancing the unfolded protein response and promoting macroautophagy. *PLoS One*. 2011;6(9):e25269.
10. Staels B, Rubenstrunk A, Noel B, et al. Hepatoprotective effects of the dual peroxisome proliferator-activated receptor alpha/delta agonist, GFT505, in rodent models of nonalcoholic fatty liver disease/nonalcoholic steatohepatitis. *Hepatology*. 2013;58(6):1941-1952.
11. Tølbøl KS, Kristiansen MNB, Hansen HH, et al. Metabolic and hepatic effects of liraglutide, obeticholic acid and elafibranor in diet-induced obese mouse models of biopsy-confirmed nonalcoholic steatohepatitis. *World J Gastroenterol*. 2018;24(2):179-194.
12. Tong W, Ju L, Qiu M, et al. Liraglutide ameliorates non-alcoholic fatty liver disease by enhancing mitochondrial architecture and promoting autophagy through the SIRT1/SIRT3-FOXO3a pathway. *Hepatol Res*. 2016;46(9):933-943.
13. Zhang L, Yang M, Ren H, et al. GLP-1 analogue prevents NAFLD in ApoE KO mice with diet and Acrp30 knockdown by inhibiting c-JNK. *Liver Int*. 2013;33(5):794-804.
14. Yan J, Yao B, Kuang H, et al. Liraglutide, sitagliptin, and insulin glargine added to metformin: the effect on body weight and intrahepatic lipid in patients with type 2 diabetes mellitus and nonalcoholic fatty liver disease. *Hepatology*. 2019;69(6):2414-2426.
15. Ratziu V, Harrison SA, Francque S, et al. Elafibranor, an agonist of the peroxisome proliferator-activated receptor-alpha and -delta, induces resolution of nonalcoholic steatohepatitis without fibrosis worsening. *Gastroenterology*. 2016;150(5):1147-1159 e1145.
16. Petit JM, Cercueil JP, Loffroy R, et al. Effect of liraglutide therapy on liver fat content in patients with inadequately controlled type 2 diabetes: the Lira-NAFLD study. *J Clin Endocrinol Metab*. 2017;102(2):407-415.
17. Mantovani A, Byrne CD, Scorletti E, Mantzoros CS, Targher G. Efficacy and safety of anti-hyperglycaemic drugs in patients with non-alcoholic fatty liver disease with or without diabetes: An updated systematic review of randomized controlled trials. *Diabetes Metab*. 2020;46(6):427-441.
18. Khoo J, Hsiang JC, Taneja R, et al. Randomized trial comparing effects of weight loss by liraglutide with lifestyle modification in non-alcoholic fatty liver disease. *Liver Int*. 2019;39(5):941-949.
19. Khoo J, Hsiang J, Taneja R, Law NM, Ang TL. Comparative effects of liraglutide 3 mg vs structured lifestyle modification on body weight, liver fat and liver function in obese patients with non-alcoholic fatty liver disease: A pilot randomized trial. *Diabetes Obes Metab*. 2017;19(12):1814-1817.
20. Cariou B, Hanf R, Lambert-Porcheron S, et al. Dual peroxisome proliferator-activated receptor alpha/delta agonist GFT505 improves hepatic and peripheral insulin sensitivity in abdominally obese subjects. *Diabetes Care*. 2013;36(10):2923-2930.
21. Armstrong MJ, Gaunt P, Aithal GP, et al. Liraglutide safety and efficacy in patients with non-alcoholic steatohepatitis (LEAN): a multicentre, double-blind, randomised, placebo-controlled phase 2 study. *Lancet*. 2016;387(10019):679-690.
22. Dufour JF, Caussy C, Loomba R. Combination therapy for non-alcoholic steatohepatitis: rationale, opportunities and challenges. *Gut*. 2020;69(10):1877-1884.
23. Perakakis N, Polyzos SA, Yazdani A, et al. Non-invasive diagnosis of non-alcoholic steatohepatitis and fibrosis with the use of omics and supervised learning: a proof of concept study. *Metabolism*. 2019;101:154005.
24. Musso G, Cassader M, Paschetta E, Gambino R. Bioactive lipid species and metabolic pathways in progression and resolution of nonalcoholic steatohepatitis. *Gastroenterology*. 2018;155(2):282-302 e288.
25. Perakakis N, Stefanakis K, Mantzoros CS. The role of omics in the pathophysiology, diagnosis and treatment of non-alcoholic fatty liver disease. *Metabolism*. 2020;111:154320.
26. Polyzos SA, Perakakis N, Boutari C, et al. Targeted analysis of three hormonal systems identifies molecules associated with the presence and severity of NAFLD. *J Clin Endocrinol Metab*. 2020;105(3):e390-e400.
27. Perakakis N, Yazdani A, Karniadakis GE, Mantzoros C. Omics, big data and machine learning as tools to propel understanding of biological mechanisms and to discover novel diagnostics and therapeutics. *Metabolism*. 2018;87:A1-A9.
28. Henderson NC, Mackinnon AC, Farnworth SL, et al. Galectin-3 regulates myofibroblast activation and hepatic fibrosis. *Proc Natl Acad Sci U S A*. 2006;103(13):5060-5065.
29. Tsuchida T, Friedman SL. Mechanisms of hepatic stellate cell activation. *Nat Rev Gastroenterol Hepatol*. 2017;14(7):397-411.
30. Kleiner DE, Brunt EM, Van Natta M, et al. Design and validation of a histological scoring system for nonalcoholic fatty liver disease. *Hepatology*. 2005;41(6):1313-1321.
31. Chong J, Xia J. MetaboAnalystR: an R package for flexible and reproducible analysis of metabolomics data. *Bioinformatics*. 2018;34(24):4313-4314.
32. Chiappini F, Coilly A, Kadar H, et al. Metabolism dysregulation induces a specific lipid signature of nonalcoholic steatohepatitis in patients. *Sci Rep*. 2017;7:46658.
33. Seebacher F, Zeigerer A, Kory N, Krahmer N. Hepatic lipid droplet homeostasis and fatty liver disease. *Semin Cell Dev Biol*. 2020;108:72-81.
34. Nathan C, SnapShot DA. Reactive oxygen intermediates (ROI). *Cell*. 2010;140(6):951-951.e2.
35. Feldstein AE, Lopez R, Tamimi T-R, et al. Mass spectrometric profiling of oxidized lipid products in human nonalcoholic fatty liver disease and nonalcoholic steatohepatitis. *J Lipid Res*. 2010;51(10):3046-3054.
36. Thompson DA, Hammock BD. Dihydroxyoctadecamonoenoate esters inhibit the neutrophil respiratory burst. *J Biosci*. 2007;32(2):279-291.
37. Armstrong MJ, Hull D, Guo K, et al. Glucagon-like peptide 1 decreases lipotoxicity in non-alcoholic steatohepatitis. *J Hepatol*. 2016;64(2):399-408.
38. Boutari C, Perakakis N, Mantzoros CS. Association of adipokines with development and progression of nonalcoholic fatty liver disease. *Endocrinol Metab (Seoul)*. 2018;33(1):33-43.
39. Li Z, Feng PP, Zhao ZB, Zhu W, Gong JP, Du HM. Liraglutide protects against inflammatory stress in non-alcoholic fatty liver by modulating Kupffer cells M2 polarization via cAMP-PKA-STAT3 signaling pathway. *Biochem Biophys Res Commun*. 2019;510(1):20-26.
40. Arab JP, Karpen SJ, Dawson PA, Arrese M, Trauner M. Bile acids and nonalcoholic fatty liver disease: molecular insights and therapeutic perspectives. *Hepatology*. 2017;65(1):350-362.

41. Lake AD, Novak P, Shipkova P, et al. Decreased hepatotoxic bile acid composition and altered synthesis in progressive human nonalcoholic fatty liver disease. *Toxicol Appl Pharmacol*. 2013;268(2):132-140.
42. Aranha MM, Cortez-Pinto H, Costa A, et al. Bile acid levels are increased in the liver of patients with steatohepatitis. *Eur J Gastroenterol Hepatol*. 2008;20(6):519-525.
43. Polyzos SA, Kountouras J, Mantzoros CS. Obeticholic acid for the treatment of nonalcoholic steatohepatitis: expectations and concerns. *Metabolism*. 2020;104:154144.
44. Holecek M. Branched-chain amino acids in health and disease: metabolism, alterations in blood plasma, and as supplements. *Nutr Metab (Lond)*. 2018;15:33.
45. Honda T, Ishigami M, Luo F, et al. Branched-chain amino acids alleviate hepatic steatosis and liver injury in choline-deficient high-fat diet induced NASH mice. *Metabolism*. 2017;69:177-187.
46. Tuccinardi D, Perakakis N, Farr OM, Upadhyay J, Mantzoros CS. Branched-Chain Amino Acids in relation to food preferences and insulin resistance in obese subjects consuming walnuts: A crossover, randomized, double-blind, placebo-controlled inpatient physiology study. *Clin Nutr*. 2021.
47. GENFIT: Announces Results from Interim Analysis of RESOLVE-IT Phase 3 Trial of Elafibranor in Adults with NASH and Fibrosis. [Web]. https://www.globenewswire.com/news-release/2020/05/11/2031418/0/en/GENFIT-Announces-Results-from-Interim-Analysis-of-RESOLVE-IT-Phase-3-Trial-of-Elafibranor-in-Adults-with-NASH-and-Fibrosis.html. Accessed Aug 16, 2020.
48. Newsome PN, Buchholtz K, Cusi K, et al. A placebo-controlled trial of subcutaneous semaglutide in nonalcoholic steatohepatitis. *N Engl J Med*. 2021;384:1113-1124.
49. Davies MJ, Bergenstal R, Bode B, et al. Efficacy of liraglutide for weight loss among patients with type 2 diabetes: the SCALE diabetes randomized clinical trial. *JAMA*. 2015;314(7):687-699.
50. Wilding JPH, Batterham RL, Calanna S, et al. Once-weekly semaglutide in adults with overweight or obesity. *N Engl J Med*. 2021;384:989-1002.

SUPPORTING INFORMATION

Additional supporting information may be found online in the Supporting Information section.

How to cite this article: Perakakis N, Stefanakis K, Feigh M, Veidal SS, Mantzoros CS. Elafibranor and liraglutide improve differentially liver health and metabolism in a mouse model of non-alcoholic steatohepatitis. *Liver Int*. 2021;41:1853–1866. https://doi.org/10.1111/liv.14888